

Genotoxicity assessment of 1,4-anhydro-4-seleno-D-talitol (SeTal) in human liver HepG2 and HepaRG cells

Raffaella di Vito^{a,1,2}, Mattia Acito^{a,1,3}, Cristina Fatigoni^{a,4}, Carl H. Schiesser^{b,5},
Michael J. Davies^{b,c,6}, Francesca Mangiavacchi^{d,7}, Milena Villarini^{a,8}, Claudio Santi^{d,9,11},
Massimo Moretti^{a,*,10,11}

^a Department of Pharmaceutical Sciences (Unit of Public Health), University of Perugia, Via del Giochetto, 06122 Perugia, Italy

^b Seleno Therapeutics Pty. Ltd., Brighton East, Victoria 3187, Australia

^c Department of Biomedical Sciences, Faculty of Health and Medical Sciences, University of Copenhagen, Blegdamsvej 3, 2200 Copenhagen, Denmark

^d Department of Pharmaceutical Sciences (Group of Catalysis Synthesis and Organic Green Chemistry), University of Perugia, Via del Liceo, 06123 Perugia, Italy

ARTICLE INFO

Handling Editor: Dr. Mathieu Vinken

Keywords:

SeTal
Cytotoxicity
Genotoxicity
Comet assay
Cytokinesis-block micronucleus test

ABSTRACT

1,4-Anhydro-4-seleno-D-talitol (SeTal) is a highly water-soluble selenosugar with interesting antioxidant and skin-tissue-repair properties; it is highly stable in simulated gastric and gastrointestinal fluids and is a potential pharmaceutical ingredient that may be administered orally. Hepatic toxicity is often a major problem with novel drugs and can result in drug withdrawal from the market. Predicting hepatotoxicity is therefore essential to minimize late failure in the drug-discovery process. Herein, we report in vitro studies to evaluate the cytotoxic and genotoxic potential of SeTal in HepG2 and hepatocyte-like differentiated HepaRG cells. Except for extremely high concentrations (10 mM, 68 h-treatment in HepG2), SeTal did not affect the viability of each cell type. While the highest examined concentrations (0.75 and 1 mM in HepG2; 1 mM in HepaRG) were observed to induce primary DNA damage, SeTal did not exhibit clastogenic or aneugenic activity toward either HepG2 or HepaRG cells. Moreover, no significant cytostasis variations were observed in any experiment. The clearly negative results observed in the CBMN test suggest that SeTal might be used as a potential active pharmaceutical ingredient. The present study will be useful for the selection of non-toxic concentrations of SeTal in future investigations.

1. Introduction

Long known for its toxicity (Carland and Fenner, 2005), selenium (Se) was recognised as an essential trace element in 1957 when Schwartz and Foltz demonstrated its protective effect against necrotic liver

degeneration in rodents and exudative diathesis in chicks (Schwarz and Foltz, 1999). Subsequently, 25 genes that code for selenoproteins have been identified in humans (Lu and Holmgren, 2009). Although many Se-containing compounds have been investigated as antioxidant (Quispel et al., 2018; Sarma and Mugesh, 2008), anticancer (Misra et al., 2015),

* Corresponding author.

E-mail addresses: raffaella.divito@outlook.it (R. di Vito), mattia.acito@unipg.it (M. Acito), cristina.fatigoni@unipg.it (C. Fatigoni), carl@selenotherapeutics.com (C.H. Schiesser), davies@sund.ku.dk (M.J. Davies), francesca.mangiavacchi@unipg.it (F. Mangiavacchi), milena.villarini@unipg.it (M. Villarini), claudio.santi@unipg.it (C. Santi), massimo.moretti@unipg.it (M. Moretti).

¹ These authors share the first authorship.

² ORCID: 0000-0003-1661-3517.

³ ORCID: 0000-0003-1808-1999.

⁴ ORCID: 0000-0002-7495-8671.

⁵ ORCID: 0000-0001-8714-1882.

⁶ ORCID: 0000-0002-5196-6919.

⁷ ORCID: 0000-0001-5344-2310.

⁸ ORCID: 0000-0002-8769-883X.

⁹ ORCID: 0000-0002-7698-8970.

¹⁰ ORCID: 0000-0002-5038-8619.

¹¹ These authors share senior and last authorship.

<https://doi.org/10.1016/j.tox.2023.153663>

Received 2 August 2023; Received in revised form 27 October 2023; Accepted 29 October 2023

Available online 2 November 2023

0300-483X/© 2023 The Authors. Published by Elsevier B.V. This is an open access article under the CC BY license (<http://creativecommons.org/licenses/by/4.0/>).

antidepressant (Victoria et al., 2014), antibiotic (Jadhav et al., 2016; Radhakrishna et al., 2010), and antiviral (Sahu et al., 2014) agents over the past few years, and the paramount biological roles that selenoproteins play, there currently are no Se-containing drugs on the market, which is partly due to selenium's tainted reputation that include murder and death by misadventure (Schiesser, 2022). Moreover, the potential therapeutic usefulness of many selenium-containing compounds is limited by their poor solubilities in aqueous media, which prevents them from reaching significant plasma concentrations (Davies and Schiesser, 2019).

To overcome the abovementioned issue, some of us have developed infinitely water-soluble selenium-containing sugars (Davies and Schiesser, 2019); these selenosugars are powerful antioxidants as evidenced by their reactivities toward hypochlorous acids, haloamines, and peroxy-nitrous acid, and typically exhibit larger rate constants than the corresponding thiosugars. Moreover, the resultant selenoxides are rapidly reduced by cellular enzyme systems and low-molecular-mass-reducing species (Carroll et al., 2017).

1,4-Anhydro-4-seleno-D-talitol (SeTal) is a novel selenosugar originally synthesized by Schiesser and co-workers (Storkey et al., 2012). This molecule exhibits intriguing antioxidant characteristics. The second-order rate constants for the reactions of SeTal with several endogenous oxidants and its antioxidant properties have been investigated. SeTal reacts rapidly with both HOCl (k $1.0 \times 10^8 \text{ M}^{-1} \text{ s}^{-1}$) and HOBr (k $1.5 \times 10^7 \text{ M}^{-1} \text{ s}^{-1}$). In addition, even though the rate constants for the reactions of SeTal with peroxy-nitrous acid/peroxy-nitrite (ONOOH/ONOO $^-$; k $2.3 \times 10^3 \text{ M}^{-1} \text{ s}^{-1}$) and chloramines (k $4.3 \times 10^2 \text{ M}^{-1} \text{ s}^{-1}$) are lower than those for hypochlorous acids, they are nevertheless larger than those of analogous thio compounds. The resulting selenoxide (SeTal(O)) is rapidly and stoichiometrically reduced by glutathione peroxidase (k $3.4 \times 10^3 \text{ M}^{-1} \text{ s}^{-1}$), using glutathione (GSH) as a co-factor, to regenerate SeTal, with concomitant formation of glutathione disulfide (GSSG). Furthermore, glutathione reductase can enzymatically reduce SeTal(O) at the expense of NADPH (Carroll et al., 2017; Carroll and Davies, 2017). Hence, endogenous antioxidant systems may be enhanced in the presence of SeTal because its oxidation–reduction cycle is rapid and highly efficient (Davies and Schiesser, 2019). In this context, SeTal has been shown to prevent the formation of 3-chlorotyrosine (3-Cl-Tyr), a biomarker of oxidative damage, in HOCl-treated human plasma (Storkey et al., 2012).

SeTal also promotes the regeneration of damaged skin tissue (Davies and Schiesser, 2019) and has been patented for that purpose (Schiesser et al., 2015). Indeed, it has been shown to prevent endothelial dysfunction caused by hyperglycaemia or by the production of O $_2^{\bullet}$, *ex vivo* in the aortae from *db/db* mice (a genetically model of obesity and diabetes). Indeed, SeTal can lead to (i) reduced O $_2^{\bullet}$ production, (ii) a higher basal NO $^{\bullet}$ level, and (iii) normalized amounts of vasoconstrictor prostanoid (Ng et al., 2017). Moreover, SeTal appears to be a privileged structure; it is more effective than other Se-containing compounds, including D,L-trans-3,4-dihydroxy-1-selenolane (DHS $_{\text{red}}$), D-selenomethionine (SeMet), its L-enantiomer, its 2*S*,3*S*,4*R*- and 2*S*,3*S*,4*S*-diastereoisomers, whereas 1,4-anhydro-D-talitol (Tal) and 1,4-anhydro-4-thio-D-talitol (STal, the sulfur analogue of SeTal) did not prevent endothelial dysfunction (Davies and Schiesser, 2019; Ng et al., 2017).

According to the above-mentioned pharmacological properties, SeTal toxicity and metabolism have been investigated in human primary coronary artery endothelial and smooth muscle cells (HCAEC and HCASMC, respectively) at concentrations up to 2 mM (Zacharias et al., 2020). Remarkably, this study reported that (i) SeTal is rapidly taken up in the intracellular compartment; (ii) SeTal does not induce any loss of metabolic activity neither after prolonged exposure, up to 16 days; (iii) SeTal does not alter cell number and growth rate of HCAEC; (iv) the selenosugar does not undergo extensive metabolism avoiding the generation of toxic metabolites (Zacharias et al., 2020).

Se-containing compounds are often characterised by poor water

solubilities. Thus, the high water/plasma solubility of SeTal is a major strength, positioning it as a suitable pharmaceutical ingredient, as its solubility will prevent tissue accumulation. In addition, it has been demonstrated that this compound is highly stable in simulated gastric and gastrointestinal fluids (Zacharias et al., 2020). This feature facilitates the oral administration of SeTal. Drugs administered by this route are typically absorbed in the gastrointestinal tract, reach the liver through the portal vein, and often undergo first-pass metabolism in this organ. Moreover, nowadays hepatic toxicity is one of the major problems causing drug withdrawals from the market (Craveiro et al., 2020; Qureshi et al., 2011) Hepatic toxicity examination is therefore a key step to avoid late-stage drug failure.

In this context, the present study aimed to analyse the *in vitro* cytotoxicity and genotoxicity of SeTal toward human hepatic HepG2 and HepaRG cells.

The findings reported here indicate that SeTal does not show hepatotoxicity except at the highest concentrations tested (0.75 and 1 mM).

2. Materials and methods

2.1. Chemical, reagents and media

Eagle's Minimum Essential Medium (MEM), William's E Medium, foetal bovine serum (FBS), Trypsin 0.25 %-EDTA 0.02 %, cytochalasin B (CytB), L-glutamine, antibiotics (penicillin and streptomycin), non-essential amino acids (NEAA), and sodium pyruvate were purchased from Euroclone SpA (Milan, Italy). Hydrochloric acid (HCl), acetic acid (AcOH), methanol (MeOH), dimethyl sulfoxide (DMSO), ethanol (EtOH), ethylenediaminetetraacetic acid disodium (Na $_2$ EDTA) and tetrasodium (Na $_4$ EDTA) salts, sodium chloride (NaCl), and sodium hydroxide (NaOH) were purchased from Carlo Erba Reagenti Srl (Milan, Italy). Dulbecco's phosphate-buffered saline w/o Ca $^{2+}$ and Mg $^{2+}$, pH 7.4 (PBS), ethidium bromide, low- and normal-melting-point agarose (LMPA and NMPA, respectively), 4-nitroquinoline-N-oxide (4-NQO), 2-amino-2-(hydroxymethyl)propane-1,3-diol (Tris-HCl), Triton X-100, hydrocortisone hemisuccinate, mitomycin C and insulin were obtained from Sigma-Aldrich Srl (Milan, Italy). Acridine orange (AO), 6,4'-diamidino-2-phenylindole (DAPI), Via1-Cassette, and NC-Slide A8 were purchased from ChemoMetec A/S (Allerød, Denmark). GlutaMAX $^{\text{TM}}$ was obtained by Thermo Fisher Scientific Inc. (Waltham, MA, USA). Conventional microscope slides and coverslips were supplied by Knittel-Glaser GmbH (Braunschweig, Germany).

2.2. SeTal synthesis

SeTal was synthesized as previously described (Mangiavacchi et al., 2020; Storkey et al., 2012). In brief, D-mannose was reacted with 2,2-dimethoxypropane in acetone in the presence of a catalytic amount *p*-toluenesulfonic acid to produce the hemiacetal, which was then reduced with sodium borohydride in methanol. The obtained diol was reacted with methanesulfonyl chloride in dichloromethane and pyridine with a catalytic amount of 4-dimethylaminopyridine (DMAP) to produce the bis-methanesulfonate intermediate. Finally, treatment with selenium and sodium borohydride in EtOH at 70 °C and deprotection using trifluoroacetic acid in dichloromethane gave SeTal, which was purified by flash chromatography.

The highest soluble concentration of SeTal for *in vitro* testing was determined according to the protocol for solubility determination proposed by the US National Toxicology Program Interagency Center for the Evaluation of Alternative Toxicological Methods (NICEATM/ICCVAM, 2006). The proposed solvents for dissolving test compounds, in the order of preference, are culture medium, DMSO, and ethanol. SeTal was freely soluble in the culture media (i.e., MEM and William's E Medium). Stock solutions (100 mM) were stored at – 20 °C until use.

2.3. Cell cultures

2.3.1. HepG2 cells

HepG2 cells were cultured in 75 cm² flasks at 37 °C, in a humidified atmosphere, in 5 % CO₂, using MEM supplemented with 10 % heat-inactivated FBS, 1 % NEAA, 1 mM sodium pyruvate, 100 U/mL penicillin, 0.1 mg/mL streptomycin. The medium culture was renewed every two to three days. When confluence (70–80 %) was achieved (normally after 48–60 h), cells were detached using 2 mL 0.25 % trypsin – 0.02 % EDTA for 5 min at 37 °C in a humidified atmosphere in 5 % CO₂, and the cell suspension was sub-cultured at a 1:2 ratio. Prior to the experiments, HepG2 cells were seeded at 2.5×10^5 cells/well in 12-well plates for the AO-DAPI viability and the comet assays, and at 5×10^5 cells/well in 6-well plates for cytokinesis block micronucleus (CBMN) assay and incubated overnight at 37 °C in a 5 %CO₂ atmosphere.

2.3.2. HepaRG

In order to obtain differentiated hepatocyte-like HepaRG cells, bipotent progenitor HepaRG cells (2×10^4 cells/cm²) were cultured in 75 cm² flasks at 37 °C, in a humidified 5 % CO₂ atmosphere using William's E Medium supplemented with 10 % heat inactivated FBS, 5 µg/mL insulin, 50 µM hydrocortisone hemisuccinate, 1 % GlutaMAX, 100 U/mL penicillin, 0.1 mg/mL streptomycin. Full confluence was achieved five days after seeding. The cells were subsequently further cultured for 10 days, during which time the confluent cells began to differentiate into hepatocytes and cholangiocytes on their own. DMSO was added at increasing concentrations (1 % for 2 days, 1.5 % for 2 days and 1.7 % until complete differentiation) to the culture medium on day fifteen to increase the expression of typical hepatocyte functions, especially CYP450 (Guillouzo et al., 2007; Laurent et al., 2013). Cells were completely differentiated 15 days after adding DMSO (Supplementary Fig. S1). The hepatocyte-like HepaRG cells were finally purified, which involved detaching cells using 2 mL of 0.25 % trypsin – 0.02 % EDTA at 37 °C for 5 min. Cell suspensions were centrifuged at 50g for 2 min, the supernatants were discarded, and pellets were resuspended in 10 mL of culture medium. The cells were finally plated in 12-well plates at high density (2×10^5 cells/cm²) to maintain their differentiated status (Supplementary Fig. S1). The medium was replaced with fresh culture medium supplemented with 1.7 % DMSO 24 h after seeding to maintain the quiescent status of the cells and facilitate full expression of hepatocyte function (Laurent et al., 2013). The medium was renewed every two days until treatment, which was carried out five days after plating. Antibiotic-free media were used for all treatments.

2.4. Assessment of cell viability: acridine orange-DAPI assay

The highest concentration of the test compounds for in vitro testing (i.e., 10 mM) was determined according to the OECD genetic toxicology test guidelines (OECD, 2015), even though 1 mM is the maximum top concentration recommended for pharmaceuticals intended for human use by the European Medicines Agency (EMA, 2012) and the US Food and Drug Administration (US FDA, 2012). Accordingly, the cells were treated with eight concentrations of SeTal (10, 5, 2.5, 1, 0.75, 0.5, 0.25, and 0.1 mM) for 4 and 68 h for HepG2, 4 and 45 h for differentiated hepatocyte-like HepaRG, with 68 (HepG2) and 45 (HepaRG) h corresponding to 1.5–2 cell cycle length (OECD, 2016, 2015). Culture medium only and culture medium supplemented with 10 % sterile MEM were used as negative controls for HepG2 and HepaRG, respectively. After treatment, the supernatant (containing floating cells) and cells were collected in 15 mL centrifuge tubes and centrifuged at 500g for 5 min. Pellets were rinsed with 1 mL PBS, centrifuged at 500g for 5 min and suspended in 1 mL PBS. Cell suspensions were transferred to 2 mL test tubes and vortexed for a few seconds. Approximately 60 µL of the sample was loaded into Via1-Cassette™ and analysed using a NucleoCounter® NC-3000™ (di Vito et al., 2022).

2.5. Assessment of primary DNA damage: comet assay

Experiments were carried out as described previously with minor modifications (Olive and Banáth, 2006; Singh et al., 1988; Villarini et al., 2021). The comet assay was carried out in triplicate using HepG2 at passages 28–34 and differentiated hepatocyte-like HepaRG at passages 12–18. In brief, HepG2 and HepaRG were challenged with the tested chemical or with 1 µM 4-NQO, as positive control. Culture medium only and culture medium supplemented with 10 % sterile MEM were used as negative controls for HepG2 and HepaRG, respectively. According to the European Medicines Agency (EMA, 2012) and the US Food and Drug Administration (US FDA, 2012), five concentrations of SeTal starting from 1 mM were tested (1, 0.75, 0.5, 0.25, and 0.1 mM).

Each supernatant was removed after 4 h of treatment at 37 °C in a 5 % CO₂ atmosphere, and the wells were rinsed twice with 0.5 mL PBS. Cells were detached using 300 µL of 0.25 % trypsin – 0.02 % EDTA (5 min at 37 °C) and 700 µL of medium culture. At the end of the treatment, viability (cell counting) was determined by AO-DAPI staining (see above) to verify that viable cells exceeded 70 %. Cell suspensions were transferred to 2 mL test tubes and centrifuged at 67g for 8 min at 4 °C. Pellets were resuspended with 0.7 % LMPA to a concentration of approximately 3×10^3 cells/µL, and 30 µL of each cell suspension was dropped onto a pre-coated (1 % NMPA) slides, covered with a coverslip and placed at 4 °C for 10 min. Two slides were set up for each sample, with each of them analysed by a different scorer. The coverslips were gently removed after 10 min and 75 µL of 0.7 % LMPA was layered and covered as described previously. Slides were placed at 4 °C for 10 min, the coverslips were removed, and the slides were placed in an ice-cold lysis solution (2.5 M NaCl, 200 mM Na₂EDTA·2 H₂O, 10 mM TRIS-HCl, pH 10.00) and left to stand overnight at 4 °C.

The slides were removed from the lysis buffer and placed in the electrophoretic chamber. DNA unwinding and electrophoresis were performed with the chamber placed in an ice bath. Electrophoretic buffer (0.3 M NaOH, 1 mM Na₄EDTA; pH > 13) was poured into the chamber to cover the slides with a thin layer. The chamber was left closed for 20 min prior to analysis to facilitate DNA unwinding. The slides were subjected to electrophoresis for 20 min (26 V, 1 V/cm; 300 mA) and then rinsed with neutralization buffer (0.4 M TRIS-HCl, pH 7.5), after which they were dehydrated by immersion in 70 % EtOH for 5 min and left to dry at room temperature.

Slides were stained with 50 µL ethidium bromide (20 µg/mL in PBS) and scored immediately by epi-fluorescence microscopy (Olympus BX41, Tokyo, Japan) under a 100 W high-pressure mercury lamp (HSH-1030-L, Ushio, Japan) at 200 × magnification. Comet images were obtained using a highly sensitive black and white CCD camera (PE2020, Pulnix Europe Ltd, Basingstoke, UK). Fifty comets were analysed for each slide using Comet Assay III® Software (Perceptive Instruments, Suffolk, UK) (Russo et al., 2020).

2.6. Assessment of cytogenetic effects: cytokinesis block micronucleus assay

Experiments were carried out in duplicate using passages 30, 33 and 34 for HepG2 and passages 8 and 17 for differentiated hepatocyte-like HepaRG. Treatment times and the protocol were in accordance with OECD/OCDE (2016) guidelines (no. 487) (OECD, 2016). In particular, two experiments were performed: (i) one with a treatment time of 4 h followed by incubation with CytB for 1.5 – 2 cell cycle lengths, and (ii) extended treatment involving both SeTal and CytB for 1.5 – 2 cell cycle lengths.

2.6.1. CBMN assay on HepG2 cells

HepG2 were seeded in 6-well plates (5×10^5 cells/well) and incubated at 37 °C in a 5 % CO₂ atmosphere overnight. The medium was removed after 18 h, the wells were rinsed with sterile PBS and then treated with five concentrations of SeTal (1; 0.75; 0.5; 0.25 and 0.1 mM).

Culture medium alone was used as the negative control, and 50 ng/mL mitomycin C was used as the positive control. The supernatants were removed after 4 h of treatment, the cells were rinsed with PBS and, due to the doubling time required for HepG2 cells (~36 h), incubated for 68 h using culture medium supplemented with 4.5 µg/mL CytB. For the extended treatment, HepG2 were treated with both SeTal and 4.5 µg/mL CytB for 68 h.

2.6.2. CBMN assay on hepatocyte-like HepaRG cells

Differentiated hepatocyte-like HepaRG were plated at a high density (2×10^5 cells/cm²) in 12-well plates and incubated at 37 °C in a 5 % CO₂ atmosphere as above described. The cells were rinsed with sterile PBS and then treated with five concentrations of SeTal (1; 0.75; 0.5; 0.25 and 0.1 mM), as described previously. Culture medium supplemented with 10 % sterile MEM was used as the negative control. The supernatants were removed after 4 h, the cells were rinsed with PBS and, due to the doubling time required for HepaRG cells (~24 h), incubated for 45 h using culture medium supplemented with 4.5 µg/mL CytB. For the extended treatment, HepaRG were treated with both SeTal and 4.5 µg/mL CytB for 45 h.

2.6.3. Cell harvesting, slide preparation and analysis

The medium was removed after treatment, the wells were rinsed twice with 0.5 mL PBS and cells were detached with 300 µL of 0.25 % trypsin – 0.02 % EDTA (5 min at 37 °C), after which 700 µL of culture medium was added to dilute trypsin and the cells were collected in Corex-glass vials and centrifuged for 5 min at 492g. A 38 µL aliquot of each sample was collected for cell counting and the viability assay, which was carried out by staining cell suspensions with 2 µL AO-DAPI solution followed by analysis using NucleoCounter® NC-3000™ in NC-Slide A8™.

The supernatants were removed after centrifugation. A 5 mL aliquot of hypotonic solution and 5 mL of cold fixative (MeOH:acetic acid, 5:1 v/v) was immediately added. Samples were centrifuged at 492g for 5 min and the pellets were resuspended using 10 mL of cold fixative and put on ice at least for 10 min. The cell suspensions were then recentrifuged, and the pellets were resuspended in fixative to a final concentration of approximately 3×10^3 cells/µL. A 60 µL sample of each cell suspension was dropped onto separate cold slides, with cells adhering firmly to the glass due to thermal shock. Two slides were prepared for each sample and separately analysed by at least two trained scorers.

Once dry, slides were immersed in staining solution (3 % GEMSA solution in 1 mM KH₂PO₄, 1 mM Na₂HPO₄ phosphate buffer) for 7 min, rinsed with distilled water and left to dry. Finally, coverslips were attached using DPX-mountant glue. Slides were scored using an Olympus BX41 (Tokyo, Japan) microscope at 400 × magnification in accordance with established criteria (Fenech, 2000; Fenech et al., 2003). Briefly, at least 2000 binucleate (BN) cells per sample have been live-scored to determine micronuclei (MN) frequency; apoptotic or necrotic cells were excluded from the analysis. Round/oval MN, not linked to the main nuclei, with a diameter between 1/3 and 1/16 and the same stain intensity of the main nuclei were counted (Supplementary Fig. S3). The MN frequency for each experimental point was expressed as micronucleate out of 1000 binucleated cells. Photomicrographs were acquired using an Optech™ camera. Afterwards, the effects of SeTal treatment on cell proliferation were estimated by calculating the cytokinesis-block proliferation index (CBPI), the replication index (RI), and the % of cytostasis (100 – RI). As indicated in the OECD guidelines, at least 1000 cells per sample were scored and classified depending on the number of nuclei in the same boundary layer, and then, the Supplementary Formulae S1 and S2 were applied (OECD, 2016).

2.7. Statistical analysis

After establishing that the data were normally distributed using the Kolmogorov-Smirnov test, they were subjected to one-way ANOVA with

Scheffé's post hoc testing to compare treated-cell and control-culture data. In AO/DAPI and in the comet assays, each value corresponds to the mean ± standard error of the mean (SEM) of at least three independent experiments (Tice et al., 2000). The CBMN assay was carried out at least in duplicate (OECD, 2016). Moreover, the test for linear trend was performed to assess the concentration-related increase in MN frequency (OECD, 2016). Data were considered significantly different at $p < 0.05$. To determine test sensitivity, cell responses to positive controls with respect to negative control cultures, were assessed using Student's *t*-test. The SPSS statistical package (SPSS Inc., Chicago, IL, USA) and GraphPad Prism software (GraphPad Software, Inc., San Diego, CA, USA) were used for statistical analyses. GraphPad Prism software was also used as the graphics program.

3. Results

3.1. Assessment of cell viability: acridine orange-DAPI assay

With the exception of extremely high concentrations (10 mM, 68 h-treatment in HepG2), treatment with SeTal did not result in a significant change in the percentage of viable cells, when compared with untreated cells (Fig. 1). Particularly, at concentrations ≤ 1 mM, average viability values were always higher than 89 %.

3.2. Assessment of primary DNA damage: comet assay

Exposure to SeTal did not give rise to significant DNA damage except at the highest examined concentrations (0.75 and 1 mM in HepG2; 1 mM in HepaRG), where a small, but significant, increase in primary DNA damage (tail intensity) was detected (Fig. 2 and Supplementary Fig. S2).

3.3. Assessment of cytogenetic effects: cytokinesis block micronucleus assay

The number of MN per 1000 binucleated cells was assessed as a measure of chromosomal abnormalities in HepG2 and HepaRG cells exposed to SeTal. None of the tested concentrations induced any statistically significant increase in the MN frequency compared with negative controls in both HepG2 and HepaRG cells (Fig. 3). Moreover, all results are inside the distribution of the historical negative control data (95 % control limits). The positive control (i.e., 50 ng/mL mitomycin C) showed the expected significant variation ($p < 0.05$), thus indicating the sensitivity of the test (Supplementary Fig. S4). The linear trend analysis also demonstrated that there is no concentration-dependent effect (HepG2 (4 h) $p = 0.338$; HepG2 (68 h) $p = 0.254$; HepaRG (4 h) $p = 0.224$; HepaRG (45 h) $p = 0.340$). Additionally, CBPI and cytostasis (%) were measured (Table 1). The CBPI is an indicator of the average number of nuclei per cell; CBPI values were determined to lie between 1.5 and 2 for both cell lines, in accordance with acceptability criteria (OECD, 2016). The cytostasis (%) calculation is performed using the RI and is indicative of the relative number of cell cycles per cell during the period of exposure to CytB in the treated culture compared to the control culture (OECD, 2016). None of the tested concentrations induced cytostasis or alteration in the CBPI in both cell lines.

4. Discussion

The present study aimed to analyse the in vitro cytotoxicity and genotoxicity of SeTal toward human hepatic HepG2 and HepaRG cells. SeTal is a new selenosugar that possesses interesting antioxidant and skin-healing properties. Indeed, it has been shown that topical application of SeTal improved, in mice, inflammatory markers, cutaneous severity scores, and scratching behaviour caused by atopic dermatitis-like cutaneous lesions induced with 2,4-dinitrochlorobenzene (Voss et al., 2021). In addition, a recent study demonstrated that the

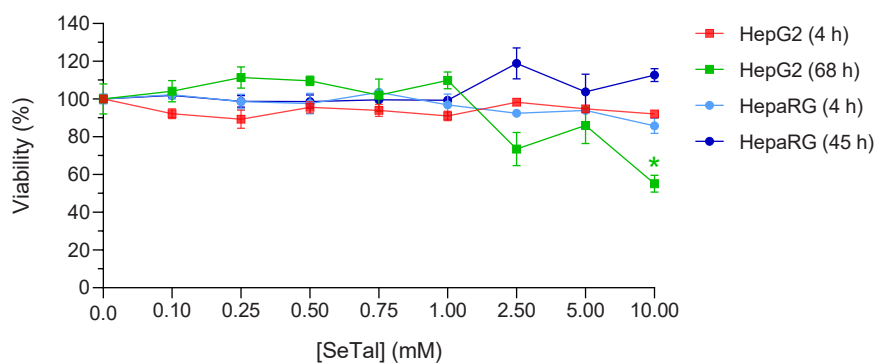


Fig. 1. Percentages of viable HepG2 and hepatocyte-like HepaRG cells after treatment with SeTal. The results are summarized as the mean (\pm SEM) of at least three independent experiments. Results are reported as variation with respect to the untreated control (taken as 100 %). Statistical analysis: one-way ANOVA followed by Scheffé's post hoc for SeTal-treated samples vs. control (untreated) cells. * $p = 0.035$.

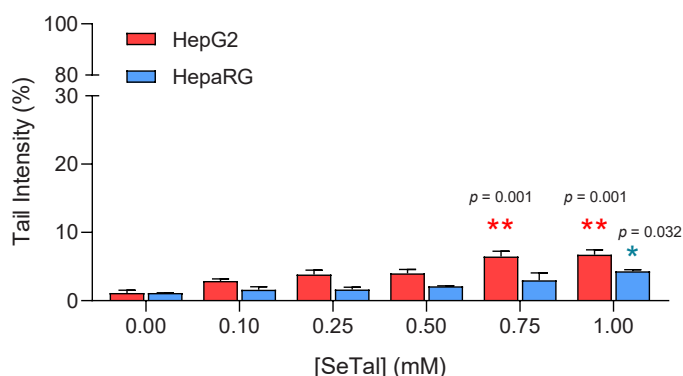


Fig. 2. Tail intensity (% DNA) was used as indicator of primary DNA damage. Results are expressed as means \pm SEM of three independent experiments. Statistical analysis: one-way ANOVA followed by Scheffé's post hoc for SeTal-treated samples vs. control (untreated) cells, * $p < 0.05$; ** $p < 0.01$. Tail intensity of positive control (1 μ M 4-NQO): HepG2 54.6 ± 0.5 ; HepaRG 23.5 ± 0.6 .

incorporation SeTal in gelatin and alginate polymeric films appears to be a promising strategy for improving the treatment and attenuation of atopic dermatitis-like symptoms in a mice model (Voss et al., 2023). Moreover, the high aqueous solubility of SeTal and its stability in simulated gastric and gastrointestinal tract fluids make it a good oral formulation candidate, and therefore examination of its hepatic toxicity is important.

In this study, AO-DAPI staining was used to evaluate the effect of SeTal on cell viability (Villarini et al., 2021), while the comet and CBMN assays were used to test the genotoxic potential of SeTal. The alkaline single-cell microgel-electrophoresis (comet) assay is a standard method for assessing the induction of primary DNA damage; it is widely used due to its simplicity, economy, sensitivity, and versatility (Collins, 2004). The comet assay facilitates the induction and observation of single- or double-strand breakage in DNA; this type of damage is often reversible because cells contain a wide range of DNA-repairing enzymes (Iyer et al., 2006; Sancar et al., 2004). Our results showed that SeTal induced a mild increase of tail intensity in 0.75 and 1 mM treated HepG2 and HepaRG exposed to 1 mM of SeTal.

On the other hand, the CBMN assay enables the clastogenic and aneugenic potentials as well as the effect on cell growth of a compound to be determined, with high reliability. OECD guidelines for this test have been published and describe their appropriate use in genotoxicity testing (OECD, 2023, 2016). MN are markers of genomic instability and originate from chromosomal breakage or whole chromosomes that, after mitosis, are not included in daughter nuclei (Hintzsche et al., 2017). Recent studies have suggested that MN might also play an active role in

tumorigenesis. Indeed, the MN nuclear envelope is fragile, and its content can be easily released in the cytosol. As a result, cytoplasmic DNA may trigger an innate pro-inflammatory response, which is commonly observed in cancer (Kwon et al., 2020). Our results suggest that SeTal is not clastogenic or aneugenic in both preclinical hepatic models. Indeed, (i) none of the tested concentrations induced a significant increase in MN frequency compared with the untreated control, (ii) there is no concentration-dependent increasing trend, and (iii) all results are inside the distribution of the historical negative control data (95 % control limits) (OECD, 2023, 2016). The reliability of our experimental model is corroborated by previous studies (Guo et al., 2020; Seo et al., 2019). Noteworthy, it has been reported that chemicals that do not require metabolic activation show similar toxicity in both HepG2 and HepaRG cells; conversely, indirect-acting genotoxicants that require metabolic activation are more effective towards differentiated hepatocyte-like HepaRG cells (Guillouzo et al., 2007; Guo et al., 2020; Seo et al., 2019). This observation is due to the different patterns of metabolic enzymes expressed in the two cell lines. Indeed, despite being metabolically competent, HepG2 cells exhibit reduced expression of drug-metabolizing enzymes, with the exception of CYP1A1 and 3A7, commonly expressed in the foetal liver (Guillouzo et al., 2007). On the contrary, the activity of phase I and II metabolizing enzymes such as CYP1A2, 2B6, 2C9, 2E1, 3A4, glutathione transferase (GST) A1/A2, GSTA4, GSTM1, and UDP-glucuronosyl transferase 1A1 was demonstrated in differentiated hepatocyte-like HepaRG (Guillouzo et al., 2007; Seo et al., 2019).

In addition, based on RI and cytostasis (%) as cytotoxicity parameters, we can conclude that SeTal is not able to alter the cell cycle and growth rate of both hepatic cell lines. This finding is in accordance with previous work on HCAEC (Zacharias et al., 2020).

Taken together, our findings suggest the non-cytotoxic and non-genotoxic nature of SeTal at concentrations ≤ 0.75 mM in hepatocyte-like HepaRG cells, and ≤ 0.5 mM in HepG2 cells. Interestingly, co-incubation of isolated mouse aortic rings with even lower concentrations (i.e., 300 μ M) of SeTal was previously shown to prevent pyrogallol-induced endothelial dysfunction (Ng et al., 2017). Accordingly, we can conclude that this bioactive concentration is also not toxic in liver cells.

In the present work, we demonstrated for the first time that SeTal appears to be a potentially active pharmaceutical ingredient at concentrations that show no hepatotoxicity. Nevertheless, the higher sensitivity of HepG2 cells compared with hepatocyte-like HepaRG cells requires further investigation; this difference is possibly due to poor HepG2 metabolism compared with the differentiated HepaRG cells, or to the potential anti-neoplastic activity of SeTal. Investigating the hepatic metabolism of SeTal, as well as its pro-apoptotic potentialities in cancer cell lines is expected to help elucidate the reason for this observation.

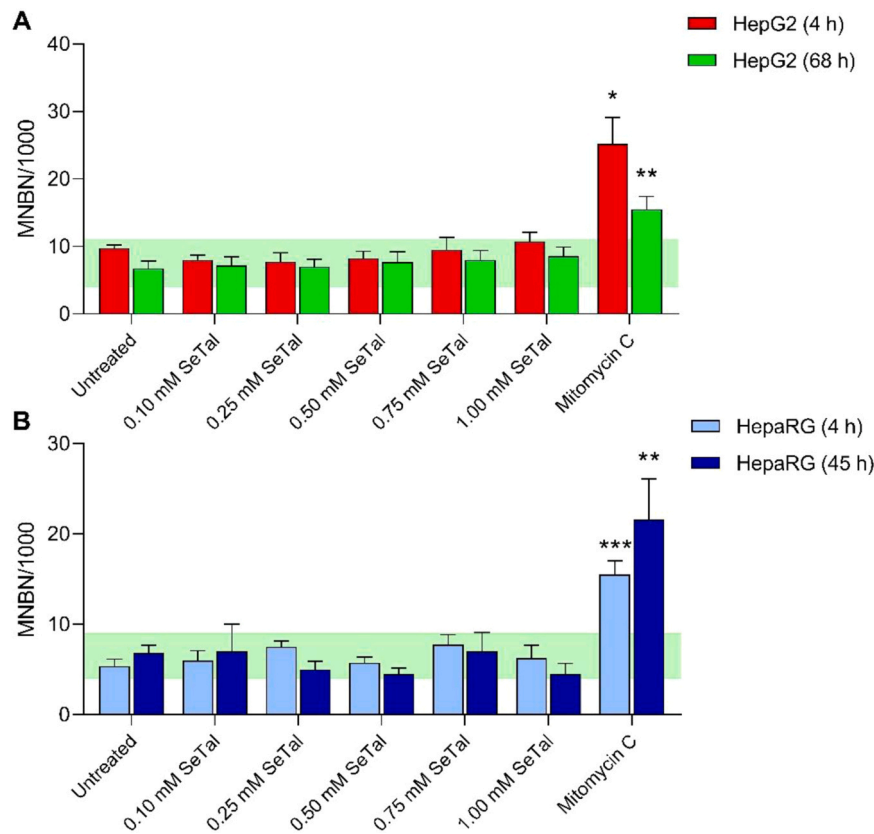


Fig. 3. Micronucleated binucleate (MNBN) cell frequency in (A) HepG2 or (B) HepaRG out of 1000 binucleate cells scored. Results are expressed as the mean \pm SEM of at least two independent experiments. The green colour indicates the 95 % control limits of the distribution of the laboratory’s historical negative control database. Statistical analysis: one-way ANOVA followed by Scheffé’s post hoc for SeTal-treated samples vs. control (untreated) cells and test for linear trend to assess the concentration-related increase of MN. Both statistical analyses did not highlight any significance. Positive control (50 ng/mL Mitomycin C) induced the expected significant increase in MN frequency: HepG2 (4 h) 25.2 ± 3.9 , $p = 0.01$; HepG2 (68 h) 15.5 ± 1.9 , $p = 0.001$; HepaRG (4 h) 15.5 ± 1.5 , $p < 0.001$; HepaRG (45 h) 21.6 ± 4.5 , $p = 0.006$ vs. negative control, Student’s *t*-test.

Table 1

Cytokinesis block proliferation index (CBPI) and cytostasis (%) in HepG2 or HepaRG cells. Results are expressed as the mean \pm SEM of two independent experiments. Statistical analysis: one-way ANOVA followed by Scheffé’s post hoc for SeTal-treated samples vs. control (untreated). Student’s *t*-test was used to compare positive vs. negative controls. * $p < 0.05$; ** $p < 0.01$.

	HepG2				Hepatocyte-like HepaRG			
	4 h		68 h		4 h		45 h	
	CBPI	Cytostasis (%)	CBPI	Cytostasis (%)	CBPI	Cytostasis (%)	CBPI	Cytostasis (%)
Untreated	1.86 \pm 0.01	0.00 \pm 0.00	1.94 \pm 0.04	0.00 \pm 0.00	1.57 \pm 0.05	0.00 \pm 0.00	1.52 \pm 0.01	0.00 \pm 0.00
SeTal 0.10 mM	1.89 \pm 0.01	-2.48 \pm 2.94	1.97 \pm 0.00	-2.90 \pm 3.31	1.51 \pm 0.01	0.02 \pm 0.02	1.54 \pm 0.01	0.67 \pm 0.67
SeTal 0.25 mM	1.86 \pm 0.01	-0.22 \pm 2.61	1.95 \pm 0.01	-0.35 \pm 2.20	1.54 \pm 0.01	0.66 \pm 1.81	1.53 \pm 0.00	0.34 \pm 0.38
SeTal 0.50 mM	1.87 \pm 0.02	-0.46 \pm 3.43	1.94 \pm 0.01	0.55 \pm 4.07	1.56 \pm 0.04	-0.14 \pm 0.22	1.52 \pm 0.00	1.49 \pm 0.70
SeTal 0.75 mM	1.87 \pm 0.04	-0.63 \pm 6.56	1.92 \pm 0.00	2.04 \pm 3.25	1.54 \pm 0.01	-0.29 \pm 0.86	1.52 \pm 0.00	0.38 \pm 0.40
SeTal 1.00 mM	1.88 \pm 0.01	-2.68 \pm 2.99	1.96 \pm 0.01	-2.18 \pm 3.00	1.53 \pm 0.01	-0.05 \pm 0.08	1.52 \pm 0.00	0.77 \pm 0.75
Mitomycin C	1.79 \pm 0.02	8.60 \pm 0.37*	1.71 \pm 0.03*	24.22 \pm 0.13**	1.53 \pm 0.01	0.18 \pm 0.96	1.56 \pm 0.03	1.47 \pm 1.84

Declaration of Competing Interest

The authors declare the following financial interests/personal relationships which may be considered as potential competing interests: Carl H. Schiesser reports a relationship with Seleno Therapeutics that includes: board membership. Michael J. Davies reports a relationship with Seleno Therapeutics that includes: board membership. Michael J. Davies and Carl H. Schiesser are major shareholders and Directors of Seleno Therapeutics, and are named as co-inventors on several patents of relevance to the work presented in this article. Michael J. Davies also declares commercial consultancy contracts with Novo Nordisk A/S. These funders had no role in the design of the study; in the collection, analyses, or interpretation of data; in the writing of the manuscript, or in

the decision to publish these results. The other authors declare no conflicts of interest with regard to the data presented.

Data availability

All data supporting the findings of this study are available within the paper and its Supplementary material.

Appendix A. Supporting information

Supplementary data associated with this article can be found in the online version at [doi:10.1016/j.tox.2023.153663](https://doi.org/10.1016/j.tox.2023.153663).

References

- Carland, M., Fenner, T., 2005. 34Se the use of selenium-based drugs in medicine. In: *Metallotherapeutic Drugs and Metal-Based Diagnostic Agents*. John Wiley & Sons, Ltd, pp. 313–332. <https://doi.org/10.1002/0470864052.ch17>.
- Carroll, L., Pattison, D.I., Fu, S., Schiesser, C.H., Davies, M.J., Hawkins, C.L., 2017. Catalytic oxidant scavenging by selenium-containing compounds: reduction of selenoxides and N-chloramines by thiols and redox enzymes. *Redox Biol.* 12, 872–882. <https://doi.org/10.1016/j.redox.2017.04.023>.
- Carroll, L.D., Davies, M.J., 2017. Chapter 9: Reaction of Selenium Compounds with Reactive Oxygen Species and the Control of Oxidative Stress. *Organoselenium Compounds in Biology and Medicine*, pp. 254–276. <https://doi.org/10.1039/9781788011907-00254>.
- Collins, A.R., 2004. The comet assay for DNA damage and repair: principles, applications, and limitations. In: *Mol. Biotechnol.*, 26, pp. 249–261. <https://doi.org/10.1385/MB:26:3:249>.
- Craveiro, N.S., Lopes, B.S., Tomás, L., Almeida, S.F., 2020. Drug withdrawal due to safety: a review of the data supporting withdrawal decision. *Curr. Drug Saf.* 15, 4–12. <https://doi.org/10.2174/1574886314666191004092520>.
- Davies, M.J., Schiesser, C.H., 2019. 1,4-Anhydro-4-seleno-D-talitol (SeTal): a remarkable selenium-containing therapeutic molecule. *New J. Chem.* 43, 9759–9765. <https://doi.org/10.1039/C9NJ02185J>.
- di Vito, R., Levorato, S., Fatigoni, C., Acito, M., Sancineto, L., Traina, G., Villarini, M., Santi, C., Moretti, M., 2022. In vitro toxicological assessment of PhSeZnCl in human liver cells. *Toxicol. Res.* <https://doi.org/10.1007/s43188-022-00148-y>.
- EMA, 2012. ICH Guideline S2(R1) Genotoxicity Testing and Data Interpretation for Pharmaceuticals Intended for Human Use (No. EMA/CHMP/ICH/126642/2008). *European Medicines Agency, Amsterdam, The Netherlands*.
- Fenech, M., 2000. The in vitro micronucleus technique. *Mutat. Res.* 455, 81–95. [https://doi.org/10.1016/S0027-5107\(00\)00065-8](https://doi.org/10.1016/S0027-5107(00)00065-8).
- Fenech, M., Chang, W.P., Kirsch-Volders, M., Holland, N., Bonassi, S., Zeiger, E., Human Micronucleus project, 2003. HUMN project: detailed description of the scoring criteria for the cytokinesis-block micronucleus assay using isolated human lymphocyte cultures. *Mutat. Res.* 534, 65–75. [https://doi.org/10.1016/S1383-5718\(02\)00249-8](https://doi.org/10.1016/S1383-5718(02)00249-8).
- Guillouzo, A., Corlu, A., Aninat, C., Glaise, D., Morel, F., Gugueng-Guillouzo, C., 2007. The human hepatoma HepaRG cells: a highly differentiated model for studies of liver metabolism and toxicity of xenobiotics. *Chem. Biol. Interact.* 168, 66–73. <https://doi.org/10.1016/j.cbi.2006.12.003>.
- Guo, X., Seo, J.-E., Petibone, D., Tryndyak, V., Lee, U.J., Zhou, T., Robison, T.W., Mei, N., 2020. Performance of HepaRG and HepG2 cells in the high-throughput micronucleus assay for in vitro genotoxicity assessment. *J. Toxicol. Environ. Health A* 83, 702–717. <https://doi.org/10.1080/15287394.2020.1822972>.
- Hintzsche, H., Hemmann, U., Poth, A., Utesch, D., Lott, J., Stopper, H., Working Group “In vitro micronucleus test”, Gesellschaft für Umwelt-Mutationsforschung (GUM, German-speaking section of the European Environmental Mutagenesis and Genomics Society EEMGS), 2017. Fate of micronuclei and micronucleated cells. *Mutat. Res. Rev. Mutat. Res.* 771, 85–98. <https://doi.org/10.1016/j.mrrev.2017.02.002>.
- Iyer, R.R., Pluciennik, A., Burdett, V., Modrich, P.L., 2006. DNA mismatch repair: functions and mechanisms. *Chem. Rev.* 106, 302–323. <https://doi.org/10.1021/cr0404794>.
- Jadhav, A.A., Dhanve, V.P., Joshi, P.G., Khanna, P.K., 2016. Solventless synthesis of new 4,5-disubstituted 1,2,3-selenadiazole derivatives and their antimicrobial studies. *Cogent Chem.* 2, 1144670. <https://doi.org/10.1080/23312009.2016.1144670>.
- Kwon, M., Leibowitz, M.L., Lee, J.-H., 2020. Small but mighty: the causes and consequences of micronucleus rupture. *Exp. Mol. Med.* 52, 1777–1786. <https://doi.org/10.1038/s12276-020-00529-z>.
- Laurent, V., Glaise, D., Nübel, T., Gilot, D., Corlu, A., Loyer, P., 2013. Highly efficient siRNA and gene transfer into hepatocyte-like HepaRG cells and primary human hepatocytes: new means for drug metabolism and toxicity studies. *Methods Mol. Biol.* 987, 295–314. https://doi.org/10.1007/978-1-62703-321-3_25.
- Lu, J., Holmgren, A., 2009. Selenoproteins. *J. Biol. Chem.* 284, 723–727. <https://doi.org/10.1074/jbc.R800045200>.
- Mangiavacchi, F., Coelho Dias, I.F., Di Lorenzo, I., Grzes, P., Palomba, M., Rosati, O., Bagnoli, L., Marini, F., Santi, C., Lenardao, E.J., Sancineto, L., 2020. Sweet selenium: synthesis and properties of selenium-containing sugars and derivatives. *Pharmaceuticals* 13, 211. <https://doi.org/10.3390/ph13090211>.
- Misra, S., Boylan, M., Selvam, A., Spallholz, J.E., Björnstedt, M., 2015. Redox-active selenium compounds—from toxicity and cell death to cancer treatment. *Nutrients* 7, 3536–3556. <https://doi.org/10.3390/nu7053536>.
- Ng, H.H., Leo, C.H., O’Sullivan, K., Alexander, S.-A., Davies, M.J., Schiesser, C.H., Parry, L.J., 2017. 1,4-Anhydro-4-seleno-d-talitol (SeTal) protects endothelial function in the mouse aorta by scavenging superoxide radicals under conditions of acute oxidative stress. *Biochem. Pharmacol.* 128, 34–45. <https://doi.org/10.1016/j.bcp.2016.12.019>.
- NICEATM/ICCVAM, 2006. Test Method Protocol for Solubility Determination; In Vitro Cytotoxicity Validation Study Phase III. National Institute of Environmental Health Sciences (NIEHS), Research Triangle Park, NC (USA).
- OECD, 2015. Guidance Document on Revisions to OECD Genetic Toxicology Test Guidelines. Organisation for Economic Co-operation and Development, Paris, France.
- OECD, 2016. Test No. 487: in Vitro Mammalian Cell Micronucleus Test. Organisation for Economic Co-operation and Development, Paris.
- OECD, 2023. Test No. 487: in Vitro Mammalian Cell Micronucleus Test. Organisation for Economic Co-operation and Development, Paris.
- Olive, P.L., Banáth, J.P., 2006. The comet assay: a method to measure DNA damage in individual cells. *Nat. Protoc.* 1, 23–29. <https://doi.org/10.1038/nprot.2006.5>.
- Quispe, R.L., Jaramillo, M.L., Galant, L.S., Engel, D., Dafre, A.L., Teixeira da Rocha, J.B., Radi, R., Farina, M., de Bem, A.F., 2018. Diphenyl diselenide protects neuronal cells against oxidative stress and mitochondrial dysfunction: Involvement of the glutathione-dependent antioxidant system. *Redox Biol.* 20, 118–129. <https://doi.org/10.1016/j.redox.2018.09.014>.
- Qureshi, Z.P., Seoane-Vazquez, E., Rodriguez-Monguio, R., Stevenson, K.B., Szeinbach, S. L., 2011. Market withdrawal of new molecular entities approved in the United States from 1980 to 2009. *Pharmacoepidemiol. Drug Saf.* 20, 772–777. <https://doi.org/10.1002/pds.2155>.
- Radhakrishna, P., K C S, M, V., Mantri, A., Mubeen, R., Kandepu, N., 2010. Synthesis and antibacterial activity of novel organoselenium compounds. *Int. J. Chem.* 2 <https://doi.org/10.5539/ijc.v2n2p149>.
- Russo, C., Acito, M., Fatigoni, C., Villarini, M., Moretti, M., 2020. B-comet assay (comet assay on buccal cells) for the evaluation of primary DNA damage in human biomonitoring studies. *Int. J. Environ. Res. Public Health* 17. <https://doi.org/10.3390/ijerph17249234>.
- Sahu, P.K., Kim, G., Yu, J., Ahn, J.Y., Song, J., Choi, Y., Jin, X., Kim, J.-H., Lee, S.K., Park, S., Jeong, L.S., 2014. Stereoselective synthesis of 4'-selenonucleosides via seleno-Michael reaction as potent antiviral agents. *Org. Lett.* 16, 5796–5799. <https://doi.org/10.1021/ol502899b>.
- Sancar, A., Lindsey-Boltz, L.A., Unsal-Kagmaz, K., Linn, S., 2004. Molecular mechanisms of mammalian DNA repair and the DNA damage checkpoints. *Annu. Rev. Biochem.* 73, 39–85. <https://doi.org/10.1146/annurev.biochem.73.011303.073723>.
- Sarma, B.K., Mughesh, G., 2008. Antioxidant activity of the anti-inflammatory compound ebelsen: a reversible cyclization pathway via selenenic and seleninic acid intermediates. *Chem. Eur. J.* 14, 10603–10614. <https://doi.org/10.1002/chem.200801258>.
- Schiesser, C., Davies, M., Storkey, C., 2015. US Patent: Selenosugars and Therapeutic Uses Thereof (Pub. No.: US 2015/0191446 A1).
- Schiesser, C.H., 2022. The quest for senocycles: from an ESR spectrum to a commercial product (17475198221089514). *J. Chem. Res.* 46 <https://doi.org/10.1177/17475198221089514>.
- Schwarz, K., Foltz, C.M., 1999. Selenium as an integral part of factor 3 against dietary necrotic liver degeneration. 1951. *Nutrition* 15, 255.
- Seo, J.-E., Tryndyak, V., Wu, Q., Dreval, K., Pogribny, I., Bryant, M., Zhou, T., Robison, T.W., Mei, N., Guo, X., 2019. Quantitative comparison of in vitro genotoxicity between metabolically competent HepaRG cells and HepG2 cells using the high-throughput high-content CometChip assay. *Arch. Toxicol.* 93, 1433–1448. <https://doi.org/10.1007/s00204-019-02406-9>.
- Singh, N.P., McCoy, M.T., Tice, R.R., Schneider, E.L., 1988. A simple technique for quantitation of low levels of DNA damage in individual cells. *Exp. Cell Res.* 175, 184–191. [https://doi.org/10.1016/0014-4827\(88\)90265-0](https://doi.org/10.1016/0014-4827(88)90265-0).
- Storkey, C., Pattison, D.L., White, J.M., Schiesser, C.H., Davies, M.J., 2012. Preventing protein oxidation with sugars: scavenging of hypohalous acids by 5-selenopyranose and 4-selenofuranose derivatives. *Chem. Res. Toxicol.* 25, 2589–2599. <https://doi.org/10.1021/tx3003593>.
- Tice, R.R., Agurell, E., Anderson, D., Burlinson, B., Hartmann, A., Kobayashi, H., Miyamae, Y., Rojas, E., Ryu, J.C., Sasaki, Y.F., 2000. Single cell gel/comet assay: guidelines for in vitro and in vivo genetic toxicology testing. *Environ. Mol. Mutagen.* 35, 206–221. [https://doi.org/10.1002/\(sici\)1098-2280\(2000\)35:3<206::aid-em3>3.0.co;2-j](https://doi.org/10.1002/(sici)1098-2280(2000)35:3<206::aid-em3>3.0.co;2-j).
- US FDA, 2012. S2(R1) Genotoxicity testing and data interpretation for pharmaceuticals intended for human use; availability. Guidance document No. Docket Number: FDA-2008-D-0178. Food and Drug Administration, Rockville, MD, USA.
- Victoria, F.N., Anversa, R., Penteado, F., Castro, M., Lenardão, E.J., Savegnago, L., 2014. Antioxidant and antidepressant-like activities of semi-synthetic α -phenylseleno citronellal. *Eur. J. Pharmacol.* 742, 131–138. <https://doi.org/10.1016/j.ejphar.2014.09.005>.
- Villarini, M., Acito, M., di Vito, R., Vannini, S., Dominici, L., Fatigoni, C., Pagiotti, R., Moretti, M., 2021. Pro-apoptotic activity of artichoke leaf extracts in human HT-29 and RKO colon cancer cells. *Int. J. Environ. Res. Public Health* 18, 4166. <https://doi.org/10.3390/ijerph18084166>.
- Voss, G.T., Davies, M.J., Schiesser, C.H., de Oliveira, R.L., Nornberg, A.B., Soares, V.R., Barcellos, A.M., Luchese, C., Fajardo, A.R., Wilhelm, E.A., 2023. Treating atopic dermatitis-like skin lesions in mice with gelatin-alginate films containing 1,4-anhydro-4-seleno-d-talitol (SeTal). *Int. J. Pharm.* 642, 123174 <https://doi.org/10.1016/j.ijpharm.2023.123174>.
- Voss, G.T., de Oliveira, R.L., Davies, M.J., Domingues, W.B., Campos, V.F., Soares, M.P., Luchese, C., Schiesser, C.H., Wilhelm, E.A., 2021. Suppressive effect of 1,4-anhydro-4-seleno-d-talitol (SeTal) on atopic dermatitis-like skin lesions in mice through regulation of inflammatory mediators. *J. Trace Elem. Med. Biol.* 67, 126795 <https://doi.org/10.1016/j.jtemb.2021.126795>.
- Zacharias, T., Flouda, K., Jepps, T.A., Gammelgaard, B., Schiesser, C.H., Davies, M.J., 2020. Effects of a novel selenium substituted-sugar (1,4-anhydro-4-seleno-d-talitol, SeTal) on human coronary artery cell lines and mouse aortic rings. *Biochem. Pharmacol.* 173, 113631 <https://doi.org/10.1016/j.bcp.2019.113631>.